

# TICAL PROPERTIES OF $p$ -TYPE $\text{Bi}_2\text{Te}_3$ - $\text{Sb}_2\text{Te}_3$ ALLOYS BETWEEN 2-15 MICRONS

R. SEHR and L. R. TESTARDI

The Franklin Institute Laboratories, Philadelphia, Pennsylvania

(Received 19 February 1962)

Transmittance and reflectance measurements have been made on a number of  $p$ -type  $\text{Te}_3$  alloys. With the electric vector in the cleavage plane, the index of refraction, energy average effective mass have been calculated. The absorption edge indicates indirect transition analysis based on phonons of a single energy is inconsistent. The reduction of the constant due to the free carrier susceptibility is observed in the alloys. In contrast to thermopiles the optical energy gaps increase with increasing Sb content, a result attributed in increasing degeneracy of the charge carriers. Temperature dependencies of the optical properties are also reported.

## INTRODUCTION

Properties of  $\text{Bi}_2\text{Te}_3$  and its alloys have been investigated in considerable detail.\* In part, these studies have been of immediate interest for the use of these materials in thermoelectric devices at room temperature. The properties of  $\text{Bi}_2\text{Te}_3$  have been investigated<sup>(1, 2)</sup> and the optical energy gaps of compounds have been reported. It appears that no work on  $\text{Sb}_2\text{Te}_3$  has been published.

Transmittance and reflectance measurements to determine the composition of the energy gap, the index of refraction, average effective mass of the charge carrier absorption and transmission. In principle the experiments provide some information on the analysis of the absorption edge to provide a consistent interpretation of the charge carriers available for this.

## EXPERIMENTAL

The samples used in this work were prepared in a soft mold (see

Appendix for partial list of references.

previous paper). Samples for optical measurements were taken from the central portions of the ingots.† For reflectance measurements the specimens were cleaved to yield, over the measured area, a mirrorlike surface with no visible stepping. Samples for transmission measurements were taken from the cleavage face of the reflectivity specimens. The sample thickness was found from mass and area measurements and the known density of the alloy compositions.<sup>(4)</sup> In the absence of visible stepping the uniformity of the thickness determined by interference fringes and sectioned sample density measurements was found adequate.

## MEASUREMENTS

Room temperature reflectance and transmittance measurements were made on a Perkin Elmer Model 21 double beam spectrometer. For low temperature transmittance measurements the single beam Model 12B with the light chopped at the source was used to avoid the wavelength dependent zero shift due to temperature differences between the sample and detector. Sample thicknesses between 4 and 12 microns were used to obtain appreciable transmission losses from absorption ( $Kd \geq 1$ ,

† The optical samples came from the same ingots as did the samples on which the transport properties, reported in the preceding paper, were measured.

with  $K$ , the absorption coefficient and  $d$  the sample thickness) while retaining a transmitted intensity of measurable magnitude.

Reflectance measurements were made at an angle slightly off normal incidence on the cleavage face of a thick specimen so that internally reflected radiation did not contribute to the observed intensity. From Fresnel's equations the slightly off normal angle of incidence generally was found to contribute a negligible error in the use of the reflectivity equation for normal incidence. The reflectance of the samples was measured relative to an aluminum reference mirror whose absolute reflectance has been reported elsewhere.<sup>(5)</sup>

If the interference fringes are not resolved the extinction coefficient,  $k$ , and the index of refraction,  $n$ , are obtained from the transmittance,  $T$ , the reflectance,  $R$ , and the sample thickness,  $d$ , by<sup>(6)</sup>

$$T = (1 - R)^2 e^{-Kd} / (1 - R^2 e^{-2Kd}) \quad (1)$$

and

$$R = \frac{(n-1)^2 + k^2}{(n+1)^2 + k^2} \quad (\text{normal incidence}), \quad (2)$$

with the absorption coefficient  $K = 4\pi k/\lambda$ . At low temperatures the reflectances were not measured and the absorption coefficient was obtained from transmission measurements on two samples of different thicknesses. In this case, to a fair approximation,  $K$  can be obtained by neglecting the second term in the denominator of equation (1).

## RESULTS

The reflectances,  $R_B$  for  $\text{Bi}_2\text{Te}_3$  and  $R_S$  for  $\text{Sb}_2\text{Te}_3$  are given in Fig. 1. Both initially decline with increasing wavelength due to the decrease in the refractive index, but for  $\text{Sb}_2\text{Te}_3$  the reflectance reaches a minimum around 9 microns and rises steeply thereafter to metallic values. This is the consequence of increasing free carrier absorption. Upon substitution of Bi for Sb in  $\text{Sb}_2\text{Te}_3$  this minimum shifts to longer wavelengths.

The index of refraction for various alloy compositions (indicated by the mol per cent  $\text{Sb}_2\text{Te}_3$ ) is given as a function of wavelength in Fig. 1. In the long wavelength region,  $n$  was obtained from equation (2) while at the shorter wavelengths more accurate values were obtained from the

interference fringes by the relation

$$2nd = N\lambda$$

where  $N$  is the order of interference. A suitable value for  $N$  was first obtained by using equation (3) using the value for  $n$  obtained

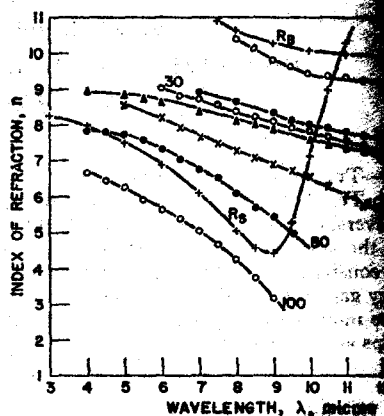


FIG. 1. Reflectance ( $R_B$  for  $\text{Bi}_2\text{Te}_3$  and  $R_S$  for  $\text{Sb}_2\text{Te}_3$ ) and index of refraction,  $n$ , for various compositions.

With the nearest integer taken as the value for  $N$ , equation (3) was applied to the fringe maxima to obtain the dielectric constant more accurately. These results generally agree within five per cent with the values obtained from reflectance and transmittance measurements.

The refractive index at a given wavelength increases with increasing Sb content. The values of  $n$  for  $\text{Bi}_2\text{Te}_3$  has been reported by AUSTIN.<sup>(1)</sup>

SPITZER and FAN<sup>(7)</sup> have shown that the contribution from the free carrier electrons to the real dielectric constant  $\epsilon$ , can be written

$$\epsilon = \epsilon_1 - \frac{Ne^2 \cdot \lambda^2}{4\pi^2 c^2 \epsilon_0 m_x^*} = n^2 - \lambda^2$$

where  $\epsilon_0$  and  $\epsilon_1$  are the dielectric constants for free space and for the material in the absence of free carriers, respectively,  $N$  is the carrier concentration,  $m_x^*$  is the effective mass of the carrier, and  $\lambda^2$  is the electric susceptibility effect. In Fig. 2 the real dielectric constant  $\epsilon$  is plotted as a function of  $\lambda^2$ . Equation (4) is well followed at the longer wavelengths (assuming  $\epsilon_1$  to be wavelength independent) while at the shorter wavelengths

results deviate from the  $\lambda^2$  behavior approaching absorption edge. The diameters of the intrinsic alloys appear to be large for all compositions although the value for  $\text{Bi}_2\text{Te}_3$ . The electric field from the large carrier concentrations in the as-grown state leads to a wavelength dependent, dielectric constant in the infrared. No simple correlation

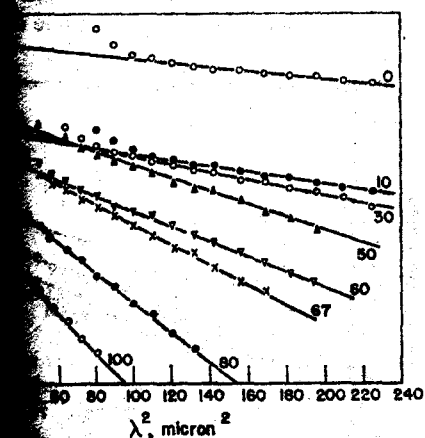


Fig. 2. Dielectric constant  $\epsilon = n^2 - k^2$  vs.  $\lambda^2$  for various alloy compositions.

reduction of the dielectric constant with the compositional dependence of the Hall coefficient indicated.

Since  $\epsilon$  vs.  $\lambda^2$ , in Fig. 2,  $m^*$  may be determined from the many valley model proposed for the band structure of  $\text{Bi}_2\text{Te}_3$  (8, 9)  $m^*$  is the inertial effective mass in the conduction band and is given as  $\alpha_1^{-1}$  in AUSTIN's model. However, the carrier concentrations  $n$  and  $N$  was replaced by the free carrier absorption coefficient,  $R_H$ , using

$$\left(\frac{\alpha_1'}{\alpha_3'}\right) \cdot \frac{\langle \tau^2 \rangle}{\langle \tau \rangle^2} \cdot \frac{1}{N e} \quad (5)$$

where  $\alpha_1^{-1}$  is the Hall coefficient anisotropy,  $\tau$  is the relaxation time averages were taken from the scattering law and Fermi level determined from the transport properties (10). With equations (4) and (5) the effective mass parameter  $(\alpha_1/\alpha_3)$  can be calculated from the carrier electric susceptibility.

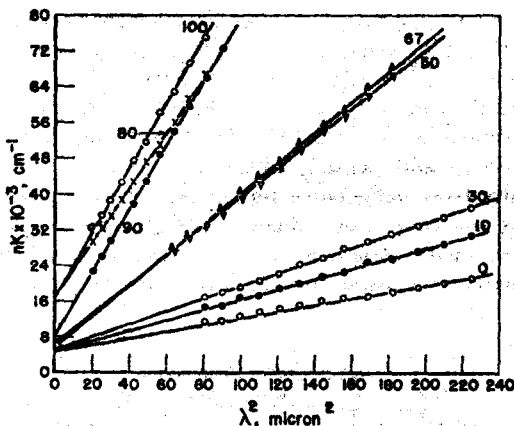


Fig. 3. Product of index of refraction and absorption coefficient,  $nK$  vs.  $\lambda^2$  for various alloy compositions.

The compositional dependence of  $(\alpha_1/\alpha_3)_X$  at 300°K is given in Fig. 4.

The same effective mass parameter evolves from the absorption coefficient measurements. With the electric vector in the cleavage planes the free carrier absorption coefficient,  $K$  is given by (10)

$$K = \frac{e^2 \lambda^2}{4 \pi^2 n e_0 m^2 c^3 \mu_H R_H} \left( \frac{\alpha_1'}{\alpha_3'} \right)_A^2 \cdot \left( \frac{\langle \tau^2 \rangle}{\langle \tau \rangle^2} \right)^2 \times \langle \tau \rangle \cdot \langle \tau^{-1} \rangle. \quad (6)$$

where  $\mu_H$  is the Hall mobility. The plot of  $nK$  for eight compositions, given in Fig. 3, shows that the desired  $\lambda^2$  dependence of the free carrier absorption

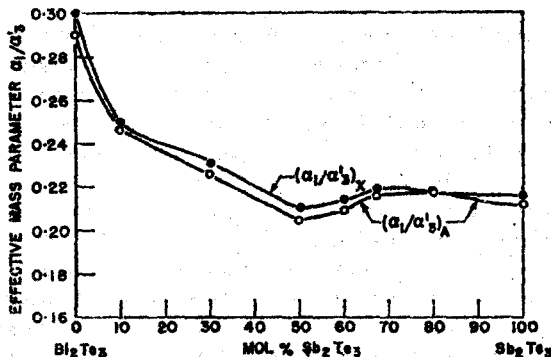


Fig. 4. The effective mass parameter  $\alpha_1/\alpha_3$  determined from free carrier susceptibility,  $(\alpha_1/\alpha_3)_X$  and from free carrier absorption,  $(\alpha_1/\alpha_3)_A$  vs. composition.

is superimposed on a broad band absorption component of undetermined origin. The effective mass parameter  $(\alpha_1/\alpha_2')_A$  obtained from equation (6) and the slopes in Fig. 3 are plotted as a function of composition in Fig. 3. The agreement between  $(\alpha_1/\alpha_2')_A$  and  $(\alpha_1/\alpha_2')_X$  which was obtained principally from reflectance measurements is to within five per cent. The values for  $\text{Bi}_2\text{Te}_3$  are in agreement with Austin's results obtained from free carrier absorption and Faraday rotation measurements.

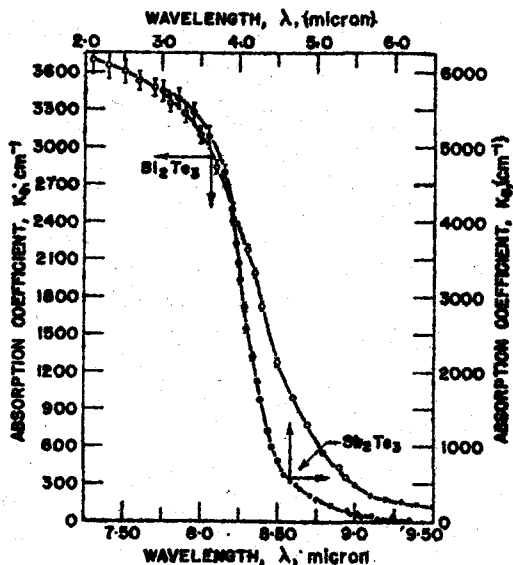


Fig. 5. Absorption coefficient,  $K$ , due to band to band transitions vs.  $\lambda$  for  $\text{Bi}_2\text{Te}_3$  and  $\text{Sb}_2\text{Te}_3$ .

With the free carrier and broad band absorption components subtracted the remaining absorption coefficient  $K_g$  was analyzed to obtain the optical energy gap and characterize the transition as direct or indirect. In Fig. 5  $K_g$  is plotted as a function of wavelength for the two extreme compositions of the alloy system. In determining the energy gap  $E_g$  we have followed Moss' criterion<sup>(11)</sup> which establishes  $E_g$  from the value of  $\lambda$  at which the slope of the absorption coefficient is a maximum. Fig. 6 gives the energy gap as a function of composition for three different temperatures. From  $\text{Bi}_2\text{Te}_3$  to 80 per cent  $\text{Sb}_2\text{Te}_3$ /20 per cent  $\text{Bi}_2\text{Te}_3$  the energy gap increases linearly with  $\text{Sb}_2\text{Te}_3$  content. The temperature coefficient of  $E_g$  is approximately

$1.5 \times 10^{-4} \text{ eV/}^\circ\text{K}$  in this range although from the increased degeneracy at lower temperatures a somewhat lower value would be expected for intrinsic semiconductors. For the very Sb rich alloys  $E_g$  rises to 0.28 eV for  $\text{Sb}_2\text{Te}_3$  at room temperature. For these compositions the Fermi level is absent of the temperature and a small temperature coefficient of  $E_g$  will be expected. For  $p$ - and  $n$ -type specimens of the Sb rich alloys an accurate

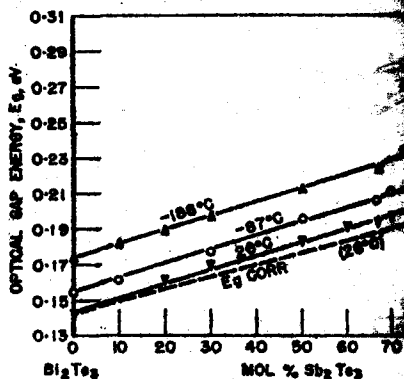


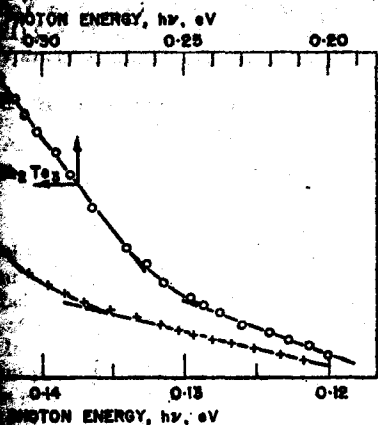
Fig. 6. Optical energy gap,  $E_g$ , vs. composition.  $E_{g \text{ corr}} = E_g (\text{observed}) - \text{Fermi level}$

of the effects of degeneracy was not least in part the increase in  $E_g$  with  $\text{Sb}_2\text{Te}_3$  content results from the increased state of degeneracy and is a situation found in  $\text{InSb}$ .<sup>(12)</sup> An estimate was provided by calculating the Fermi level from the observed Seebeck coefficient. The  $E_{g \text{ corr}}$  have been plotted in Fig. 6 as  $E_{g \text{ corr}}$ . The transitions were direct an additional  $E_g$  would be associated with the density of states effective masses for electrons. The bulk of the experimental data, however, indicates indirect transitions.

The absorption edges of several alloys were analyzed to determine whether the transition was direct or indirect. Generally,  $K_g$  vs.  $h\nu$  where  $h\nu$  is the incident photon energy, is  $\propto h\nu - E_g$  for direct transitions and  $\propto (h\nu - E_g)^2$  for indirect transitions. Our data are consistent with  $n = 2$  as shown in Fig. 7 for  $\text{Bi}_2\text{Te}_3$  and  $\text{Sb}_2\text{Te}_3$ . In both cases the plot of  $K_g^{1/2}$  vs.  $h\nu$

as predicted for indirect transition expression of MACFARLANE and

$$\frac{(E_g - \hbar\theta)^2}{\exp(-\theta/T)} + \frac{(\hbar\nu - E_g + \hbar\theta)^2}{\exp(\theta/T) - 1} \quad (7)$$



Plot of absorption coefficient,  $K_{1/2}$ , vs. photon energy for  $\text{Bi}_2\text{Te}_3$  and  $\text{Sb}_2\text{Te}_3$ .

phonon energy necessary to con-  
The first term corresponds to  
and the second to phonon absorp-  
equation to our results at room  
obtain from the intercepts  $\hbar\theta$   
and 400°K and  $E_g$  equal to 0.13 eV  
 $\text{Bi}_2\text{Te}_3$  and  $\text{Sb}_2\text{Te}_3$  respectively.  
ing values of  $\hbar\theta$  from the slopes,  
but three and four times larger,  
similar discrepancy for  $\text{Bi}_2\text{Te}_3$  has  
AUSTIN.<sup>(1)</sup> Although equation (7)  
for degeneracy this should be  
 $\text{Bi}_2\text{Te}_3$ . Ignoring the modification  
by degeneracy the optical energy  
for indirect transitions from the  
7 are smaller than those obtained  
(Fig. 6). This result, together  
of degeneracy, will account at  
apparent discrepancy between  
energy gaps. Values for the  
gaps from high temperature re-  
sults have been obtained in this  
results show an energy gap of  
which decreases on alloying to  
70 per cent  $\text{Sb}_2\text{Te}_3$ /30 per cent

$\text{Bi}_2\text{Te}_3$ . With increasing degeneracy our optical and thermal measurements would tend, respectively, to overestimate and underestimate the energy gap. For the very Sb rich compositions (including  $\text{Sb}_2\text{Te}_3$ ) the strong degeneracy led to resistivity maxima at temperatures too close to the melting points to permit a determination of  $E_g$ . Attempts at compensation were unsuccessful.

## CONCLUSIONS

The infrared studies have shown that most of the alloy system is characterized by a large dielectric constant although the effects of the free carrier susceptibility are quite marked for the more degenerate alloys. For the larger part the optical behavior was in agreement with the predictions of the Drude-Zener theory. An effective mass average obtained from electric susceptibility and free carrier absorption measurements is reported but more work is needed to establish the band structure parameters completely.

Evidence obtained from measurements of the transport properties indicate the effective mass to be insensitive to variations in carrier concentration or degeneracy, at least over changes in these two variables as occur in the as-grown materials. Although exact carrier concentrations cannot be obtained from Hall measurements without further knowledge of the band structure, it is estimated that a hole concentration in excess of  $10^{19} \text{ cm}^{-3}$  occurred in most of the alloys. A possible reason for independence of the effective mass on hole concentration at such levels seems to be the very large dielectric constant screening of the crystalline field. In a calculation for heavily doped Germanium CONWELL and SCHLOSSER<sup>(14)</sup> arrive at a similar conclusion.

In the analysis of the absorption edge the transitions appear as indirect but no satisfactory account was made of the effects of degeneracy. At least in the compositional range  $\text{Bi}_2\text{Te}_3$  to 70 per cent  $\text{Sb}_2\text{Te}_3$ /30 per cent  $\text{Bi}_2\text{Te}_3$  the energy gap should fall somewhere between the optical and thermal values and, therefore, does not vary to a great extent with composition.

**Acknowledgements**—The authors wish to thank Mr. G. K. McCONNELL for his valuable aid in the experimental work and the sponsors of the Thermoelectric Effects Research Program for their financial support.

## REFERENCES

1. AUSTIN I. G., *Proc. phys. Soc. Lond.* **72**, 545 (1958).
2. AUSTIN I. G., *Proc. phys. Soc. Lond.* **76**, 169 (1960).
3. BLACK J., CONWELL E. M., SEIGLE L. and SPENCER C. W., *J. Phys. Chem. Solids* **2**, 240 (1957).
4. TESTARDI L. R. and WIESE J. R., *Trans. Amer. Inst. min. (metall.) Engrs.* **221**, 646 (1961).
5. HASS G., *J. opt. Soc. Amer.* **45**, 945 (1955).
6. BECKER M. and FAN H. Y., *Phys. Rev.* **76**, 1530 (1949).
7. SPITZER W. G. and FAN H. Y., *Phys. Rev.* **106**, 882 (1957).
8. DRABBLE J. R. and WOLFE R., *Proc. Roy. Soc. Lond.* **B69**, 1101 (1956).
9. DRABBLE J. R., *Proc. phys. Soc.* (1958).
10. AUSTIN I. G., *J. Electron. Cont.* **5**, 1 (1958).
11. MOSS T. S., *Optical Properties of Semiconductors*, p. 40. Academic Press, New York (1956).
12. BURSTEIN E., *Phys. Rev.* **93**, 632 (1954).
13. MACFARLANE G. G. and ROBERTS V., *Phys. Rev.* **100**, 1714 (1955).
14. CONWELL E. M., SCHLOSSER H., *Phys. Rev.* **125**, 214 (1962).